Controllers Comparison to stabilize a Two-wheeled Inverted Pendulum: PID, LQR and Sliding Mode Control

JUAN VILLACRÉS[1], MICHELLE VISCAINO[1], MARCO HERRERA[1], OSCAR CAMACHO[1, 2]
[1] Departamento de Automatización y Control Industrial, Facultad de Ingeniería Eléctrica y Electrónica. Escuela Politécnica Nacional, Quito. ECUADOR
[2] Facultad de Ingeniería. Universidad de los Andes. Mérida. VENEZUELA
{juan.villacres01; michelle.viscaino; marco.herrera; oscar.camacho}@epn.edu.ec, ocamacho@ula.ve

Abstract: -This paper compares three control strategies to stabilize a two-wheeled inverted pendulum (TWIP). The study of TWIP or balancing robot has been extensive because of its unstable and multivariable nature with highly non-linear dynamics. The mathematical model was derived using Lagrangian approach and was linearized around the equilibrium point where was considered that the pitch angle tends to zero. The study used a classic PID control, a Linear-Quadratic Regulator (LQR) and a Slide Mode Control (SMC). The SMC part of state-space representation of the system and the slide surface was designed from the poles obtained from LQR, therefore design an Optimal SMC. All the close-loop controllers are in discrete-time; therefore, they were implemented in a digital way. The results were obtained by simulation using Matlab. The stabilization results were compared in terms of disturbances rejection capability and the integral square error (ISE) is used to measure their performance.

Key-Words: - **Two-Wheeled Inverted Pendulum, Sliding Mode Control, LQR, stabilization, Lagrangian approach**

1 Introduction

In the early 60s, several laboratories of prestigious universities [1] guided and made experiments which showed a rod mounted on a carriage, if the rod is placed in an upright position manually, it could maintain its position autonomously by the action of the vehicle displacement on which it is stood. This mechanism would represent an unstable open loop system with nonlinear dynamics which can be interpreted by differential equations; therefore, inverted pendulum control to maintain its vertical position independently became a classic problem of nonlinear control. [2] [3]

This platform has been a great help in research to test the effectiveness of different control techniques on a nonlinear system with unstable dynamic. Additionally, it presents feature of an underactuated system difficult to apply conventional approaches to robotics [4].

Several works have studied different control strategies that have been applied to this kind of systems. In [4], a dynamic model was derived using a Newtonian approach and presented a comparison of LQR and PID-PID input in terms of tracking and disturbances.

In [5], a dynamic model was derived using a Newtonian approach and two decoupled state-space controllers around an operating point to design a system control. In [6] sliding mode control for robust velocity eliminating the steady velocity tracking error is designed. In [7], a dynamic model was derived using Lagrangian approach, two-level velocity controllers via partial feedback linearization and stabilizing position were designed.

This paper compares three control strategies to stabilize a two-wheeled inverted pendulum (TWIP). As it was mentioned, the study of TWIP or balancing robot has been extensive because of its unstable nature with highly non-linear dynamics. The paper begins with an introduction, the second section provides an explanation of the model under study, in the third section basic concepts of control strategies employed are described and the design of PID, LQR and SMC are developed, the fourth section presents the simulation results with a performance analysis based on ISE criterion for each control technique, and finally the conclusions are presented.

2 Description of the Two Wheeled Inverted Pendulum

By rotating the wheels in an appropriate direction TWIP balance is stable. For stabilization the control actions are carried out in micro-electromechanical with a sampling frequency of 100 Hz. The signals required are obtained from a sensor gyroscope who measures angular velocity and angular position by estimating of the pendulum in the vertical plane. The measure of the angle rotation of each wheel is obtained by encoders localized at each wheel in the robot body. The motors DC are controlled by a signal Pulse Width Modulated (PWM). [15]

The system receives as inputs the voltages of each spare tire (u_l and u_d) and its outputs are the body pitch angle ψ [rad], the average angular position of the wheels θ [rad] and their velocities $\dot{\psi}$ [rad/s], $\dot{\theta}$ [rad/s], in Fig.1 is shown.

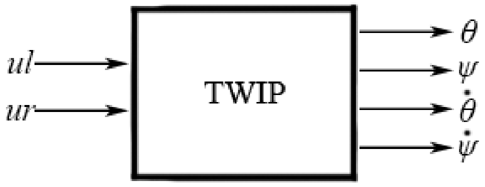

Fig. 1 Input/output Scheme of TWIP

In Fig. 2 the variables of the system are shown.

ψ: Body pitch angle.
θ: Average angular position (right and left).
ϕ: Body yaw angle.

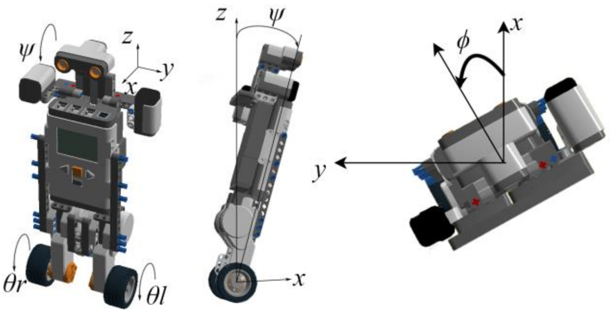

Fig. 2 System Views: Frontal, lateral and top

2.1 Model of Two-Wheeled Inverted Pendulum

The system's model is taken from [9], TWIP is described with nonlinear differential equations obtained by Lagrange method, and the model is linearized around an equilibrium point where the body pitch angle tends to zero.
The model is represented in space state:

$$\dot{x}_1 = A_1 x_1 + B_1 u \tag{1}$$

Where:

$$x_1 = \begin{bmatrix} \theta \\ \psi \\ \dot{\theta} \\ \dot{\psi} \end{bmatrix} \tag{2}$$

$$u = \begin{bmatrix} u_l \\ u_r \end{bmatrix} \tag{3}$$

$$A_1 = \begin{bmatrix} 0 & 0 & 1 & 0 \\ 0 & 0 & 0 & 1 \\ 0 & a_{32} & a_{33} & a_{34} \\ 0 & a_{42} & a_{43} & a_{44} \end{bmatrix} \tag{4}$$

$$B_1 = \begin{bmatrix} 0 & 0 \\ 0 & 0 \\ b_3 & b_3 \\ b_4 & b_4 \end{bmatrix} \tag{5}$$

Where:

$$a_{32} = -gMLe_{12}/\det(E) \tag{6}$$
$$a_{42} = gMLe_{11}/\det(E) \tag{7}$$
$$a_{33} = -2(\sigma e_{22} + \beta e_{12})/\det(E) \tag{8}$$
$$a_{43} = 2(\sigma e_{12} + \beta e_{11})/\det(E) \tag{9}$$
$$a_{34} = 2\beta(e_{22} + e_{12})/\det(E) \tag{10}$$
$$a_{44} = -2\beta(e_{11} + e_{12})/\det(E) \tag{11}$$
$$b_3 = \alpha(e_{22} + e_{12})/\det(E) \tag{12}$$
$$b_4 = -\alpha(e_{11} + e_{12})/\det(E) \tag{13}$$
$$e_{11} = (2m + M)R^2 + 2J_w + 2n^2 J_m \tag{14}$$
$$e_{12} = MLR - 2n^2 J_m \tag{15}$$
$$e_{22} = ML^2 + J_\psi + 2n^2 J_m \tag{16}$$

$$\det(E) = e_{11}e_{22} - e_{12}^2 \tag{17}$$

$$\alpha = nK_t/R_m \tag{18}$$
$$\beta = nK_t K_b/R_m + f_m \tag{19}$$
$$\sigma = \beta + f_w \tag{20}$$

The parameter values are described in Table 1; they were taken from [10].

Table 1. Parameter of TWIP

Parameter	Unit	Description
$g = 9.8$	$[m/sec^2]$	Gravity acceleration
$m = 0.03$	$[kg]$	Wheel mass
$R = 0.021$	$[m]$	Wheel radius
$J_w = mR^2/2$	$[kgm^2]$	Wheel inertia moment
$M = 0.6$	$[kg]$	Body mass
$W = 0.09$	$[m]$	Body width
$D = 0.05$	$[m]$	Body depth
$H = 0.26$	$[m]$	Body height
$L = H/2$	$[m]$	Distance of the center of the mass from the Wheel axle
$J_\psi = ML^2/3$	$[kgm^2]$	Body pitch inertia moment
$J_\phi = M(W^2 + D^2)/12$	$[kgm^2]$	Body yaw inertia moment
$J_m = 1x10^{-5}$	$[kgm^2]$	DC motor inertia moment

$R_m = 6.69$	$[\Omega]$	DC motor resistance
$K_b = 0.468$	[V sec /rad]	DC motor back e.m.f constant
$K_t = 0.317$	[Nm/A]	DC motor torque constant
$n = 1$	Gear ratio	
$f_m = 0.0022$	Friction coefficient between body and DC motor	
$f_w = 0$	Friction coefficient between body and motion surface	

Replacing the parameter values of Table1 in the equation from (4) to (20). The following matrices are obtained:

$$A_1(t) = \begin{bmatrix} 0 & 0 & 1 & 0 \\ 0 & 0 & 0 & 1 \\ 0 & -698.30 & -416.80 & 416.80 \\ 0 & 139.96 & 53.41 & -53.41 \end{bmatrix} \tag{21}$$

$$B_1(t) = \begin{bmatrix} 0 & 0 \\ 0 & 0 \\ 405.11 & 405.11 \\ -51.91 & -51.91 \end{bmatrix} \tag{22}$$

In order to design the discrete controllers, the continuous-time system is converted into a discrete-time system, with the next equations: [3]

$$A_d = e^{A_c T_o} \tag{23}$$

$$B_d = A_c^{-1}(A_d - I)B_c \tag{24}$$

Where:

A_c: Continuous-time State matrix
B_c: Continuous-time Input matrix
A_d: Discrete-time State matrix
B_d: Discrete -time Input matrix
T_0: Sampling time

Replacing equations (21) and (22) into equations (23) and (24), with $T_0 = 10$ ms, the following matrices are found:

$$A[k] = \begin{bmatrix} 1 & -0.010 & 0.003 & 0.007 \\ 0 & 1.004 & 0.0009 & 0.0091 \\ 0 & -1.122 & 0.1207 & 0.8690 \\ 0 & 0.649 & 0.1129 & 0.8910 \end{bmatrix} \tag{25}$$

$$B[k] = \begin{bmatrix} 0.0068 & 0.0068 \\ -0.0009 & -0.0009 \\ 0.8546 & 0.8546 \\ -0.1097 & -0.1097 \end{bmatrix} \tag{26}$$

The open-loop poles for the discrete-time system are:

$$p_1 = 1 \tag{27}$$
$$p_2 = 0.0091 \tag{28}$$
$$p_3 = 1.0703 \tag{29}$$
$$p_4 = 0.9362 \tag{30}$$

In equation (27) the pole is on the unit circle while in (29) the pole is outside the unit circle, which evidences the instability of the system in open-loop.

3 Controllers

In this section, three strategies of control are developed. The controllers are used to stabilize the Two-Wheeled Inverted Pendulum. The controllers developed and later compared are: A classic PID controller, an optimal LQR regulator and a Slide Mode Controller.

3.1 PID

The continuous PID (31) must be discretized. For the integral component the trapezoidal integration and for the derivative component the forward integration are used, the equation is given as (32). [11]

$$G_c = K_P + K_D s + \frac{K_I}{s} \tag{31}$$

$$\frac{U(z)}{E(z)} = k_p + k_i\left(\frac{T_0}{2}\frac{z+1}{z-1}\right) + K_d\left(\frac{1}{T_0}\frac{z-1}{z}\right) \tag{32}$$

Applying the inverse Z transform (33) into (32), (34) is obtained.

$$z^{-n}F(z) = F(k-n) \tag{33}$$

$$u(k) = u(k-1) + E(k)\left(K_P + \frac{K_I T_0}{2} + \frac{K_D}{T_0}\right) + E(k-1)\left(-K_P + \frac{K_I T_0}{2} - \frac{2K_D}{T_0}\right) + E(k-2)\left(\frac{K_D}{T_0}\right) \tag{34}$$

And:

$$E(k) = x_{ref}(k) - x(k) \tag{35}$$

Where:
x_{ref}: It represents the desired states, in this case to stabilize the TWIP the $x_{ref} = 0$.
x: It represents the value of the system outputs.

Two PID controllers are designed. The first PID controller designed is the one who controls the body pitch angle. The second PID controller designed is the one which controls the angular position of the wheels.

The parameters of the PID controllers are obtained by trial and error. The tuned parameters are given as in table 2.

Table 2. PID parameters

	K_P	K_I	K_D
ψ	-77.97	-0.01	-8.79
θ	-1.07	-0.01	-1.36

3.2 LQR

The Linear Quadratic Regulator is a state feedback control which is useful to handle multivariable systems.
It is assumed that the system is given by the following equation:

$$x(k+1) = Ax(k) + Bu(k) \tag{36}$$

The input for the system will be:

$$u(k) = -Kx(k) \tag{37}$$

Where K is the gain matrix. The matrix K has to bring the system into a final state $x(k_1) = 0$ from an initial state $x(k_0)$.
To determine the matrix K, the performance index should be minimized.

$$J = \sum_{k=k_0}^{k_1-1} x^T(k+1)Qx(k+1) + u^T(k)Ru(k) \tag{38}$$

Where:
$Q \in \mathbb{R}^{nxn}$: It is a symmetric matrix, at least positive semidefinite.
$R \in \mathbb{R}^{mxm}$: It is a symmetric matrix positive semidefinite.
Replacing (37) into (36):

$$x(k+1) = Ax(k) - BKx(k) = (A - BK)x(k) \tag{39}$$

In order to solve the equation (38), the Optimality Principle [10] is used:

$$K(i) = [R + B^T P(i+1)B)^{-1} B^T P(i+1)A \tag{40}$$

$$P(i) = Q + K^T(i)RK(i) + [A - BK(i)^T P(i+1)[A - BK(i)] \tag{41}$$

The iterative calculation begins with $P(N) = Q$ y $K(N) = 0$ from $u(N-1)$ until $u(0)$.
This iterative sequence converges when $N \to \infty$
The objective is to verify the convergence of the matrix K.

$$\|K_N - K_{N-1}\| < \frac{\gamma}{\|K_N\|} \tag{42}$$

Where:
γ: It is a parameter which allows calibrate the convergence condition.

The matrices Q and R selected are:

$$Q = \begin{bmatrix} 0.38 & 0 & 0 & 0 \\ 0 & 0.43 & 0 & 0 \\ 0 & 0 & 0.09 & 0 \\ 0 & 0 & 0 & 0.09 \end{bmatrix} \tag{43}$$

$$R = \begin{bmatrix} 0.00017 & 0 \\ 0 & 0.00017 \end{bmatrix} \tag{44}$$

The matrix K obtained is:

$$K = \begin{bmatrix} -1.099 & -81.44 & -1.368 & -10.860 \\ -1.099 & -81.44 & -1.368 & -10.860 \end{bmatrix} \tag{45}$$

3.3 Slide Mode Control (SMC)

It is assumed that the system is given by the following equation:

$$x(k+1) = Ax(k) + Bu(k) \tag{46}$$

It is supposed that the pair (A, B) is controllable, therefore, there is a non-singular matrix $T \in \mathbb{R}^{nxn}$ which makes the system in its controllable canonical form. [12-13]

$$\bar{x}(k+1) = \bar{A}\bar{x}(k) + \bar{B}u(k) \tag{47}$$

Where:

$$\bar{A} = T_1^{-1} A T_1 \tag{48}$$

$$\bar{B} = T^{-1} B \tag{49}$$

It is defined a linear function, called sliding surface:

$$s(x(k)) = Sx(k) = \bar{S}\bar{x}(k) \qquad \bar{S} \in \mathbb{R}^{1xn} \tag{50}$$

Where: $\bar{S} = ST_1$ (51)

$$\bar{S} = [\bar{s}_1 \quad \bar{s}_2 \quad \dots \quad \bar{s}_{n-1} \quad 1] \tag{52}$$

Thus, the design of the sliding mode for the reduced order system defined by (53) is stable. [12-13]

$$s(x(k)) = \bar{S}\bar{x}(k) = 0 \tag{53}$$

$$S\bar{x}(k) = \bar{s}_1 y + \bar{s}_2 y^k + \dots + \bar{s}_{n-1} y^{k(n-2)} + y^{k(n-1)} = 0 \tag{54}$$

The equivalent control must guarantee that:

$$Sx(k+1) = 0 \tag{55}$$

$$Sx(k+1) = S\left(Ax(k) + Bu_{eq}(k)\right) = 0 \tag{56}$$

So,

$$u_{eq}(k) = -(SB)^{-1}SAx(k) \tag{57}$$

The control law (58) has two components, a continuous one $u_{eq}(k)$ and a discontinuous one v.

$$u(k) = u_{eq}(k) + v \tag{58}$$

In order to achieve steady state equal to zero: [12]

$$v = \begin{cases} cte, & s(x) < 0 \\ 0, & s(x) = 0 \\ -cte, & s(x) > 0 \end{cases} \tag{59}$$

To design the slide surface, the new poles (60), (61) obtained from feedback the matrix K (45) are: [13]

$$p1{,}2 = 0.9318 \pm 0.0042i \tag{60}$$
$$p3 = 0.9797 \tag{61}$$

With these poles, the slide surface obtained is given by:

$$s(x(k)) = [-1.924 \quad -147.918 \quad -1.669 \quad -21.065] \tag{62}$$

And the equivalent control law is:

$$u_{eq}(k) = [1.924 \quad 160.270 \quad 2.717 \quad 21.581] \tag{63}$$

To reduce the chattering produced by high frequency switching, a filter for chattering reduction is used [14], the filter is shown in fig.3 described by (64)

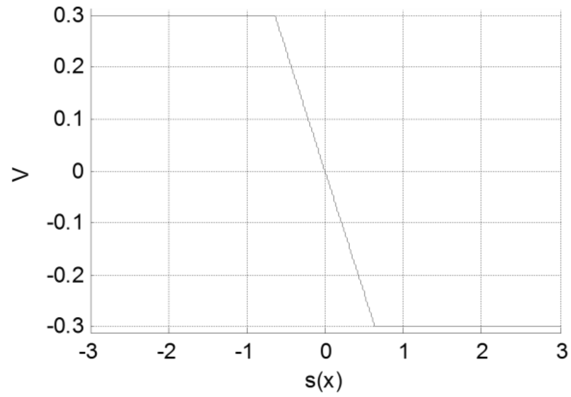

Fig. 3 Filter for chattering reduction

$$v = \begin{cases} cte, & s(x(k)) < L \\ -\frac{s}{L}, & |s(x(k))| \le L \\ -cte, & s(x(k)) > L \end{cases} \tag{64}$$

4 Simulation Results

In this section, the performance of the three controllers is compared. The simulations are performed by using Simulink-Matlab.

The simulation scheme is similar for the controllers, as shown in fig. 4, where a sampler and zero-order holder are used in order to simulate a discrete-time system.

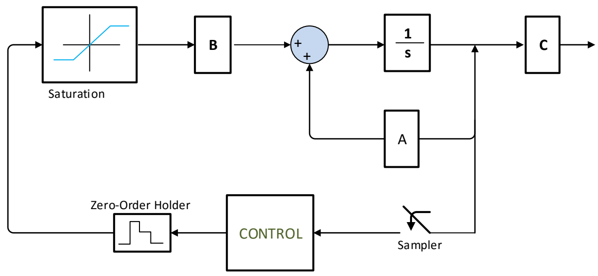

Fig. 4 Linear System and Control scheme

As it had been indicated the states of TWIP are $x = [\theta \quad \psi \quad \dot{\theta} \quad \dot{\psi}]^T$. The main purpose of the control is to keep the TWIP in a vertical position.

4.1 Simulations with initial conditions and without any disturbance

Assuming that the initial states are:

$$x_o = [0 \quad 0.1 \quad 0 \quad 0]^T \tag{65}$$

The next figures show the responses, when each controller is used.

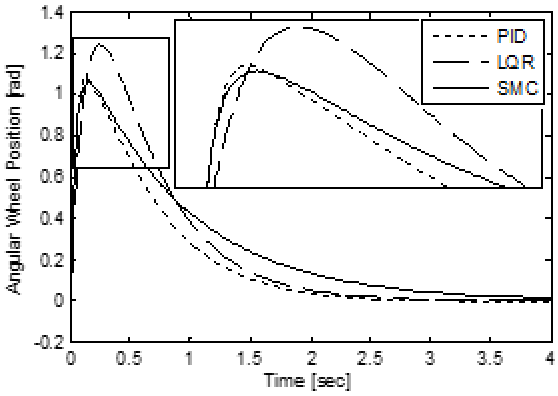

Fig. 5 TWIP, angular wheel position response

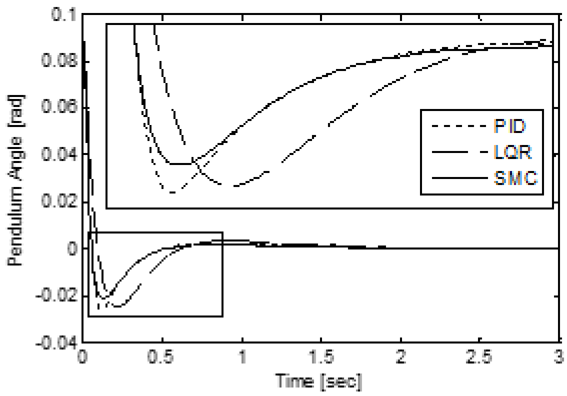

Fig. 6 TWIP, body pitch angle response

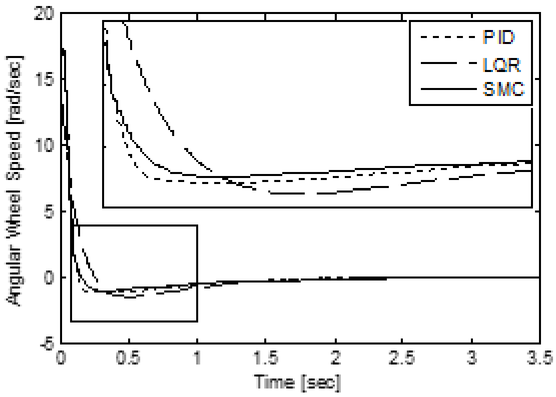

Fig. 7 TWIP, angular wheel speed response

According with the fig. 6, the SMC presents a smooth response to stabilize the body pitch angle. The three controllers have similar settling time as shown in fig. 5. To stabilize the body pitch angle the SMC has the lowest value of ISE, but to get steady state of the angular wheel position, the PID has the lowest value of ISE as shown in table 3.

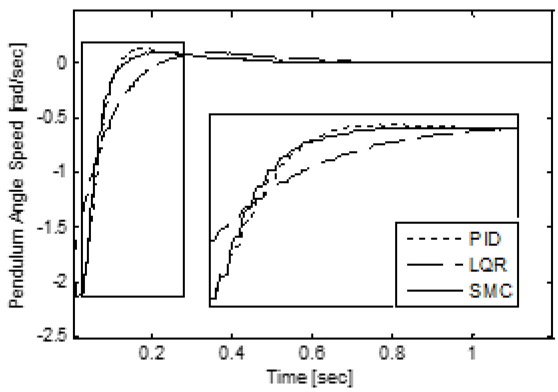

Fig. 8 TWIP, body pitch angle speed response

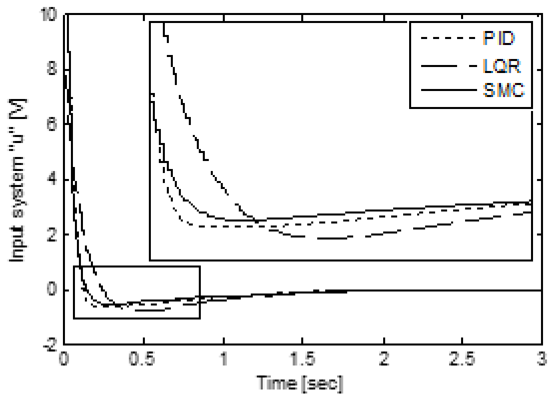

Fig. 9 TWIP, input system u

In fig. 9, it is shown that LQR uses less energy, at the start than the others.

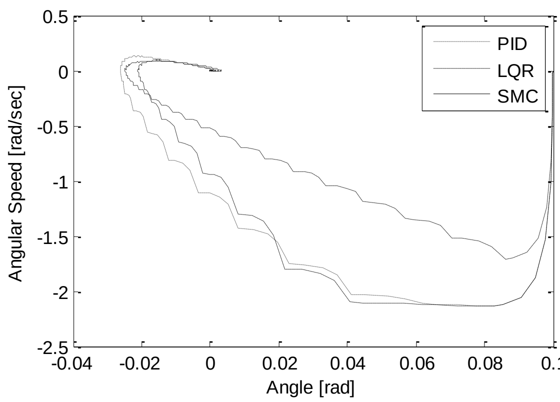

Fig. 10 TWIP, Phase Portrait body pitch angle

Table 3. ISE Comparison of three controllers without disturbance

	PID	LQR	SMC
	ISE $* 10^{-3}$		
ψ	0.271	0.393	0.247
θ	526.6	810	660.9

4.2 Simulations with initial conditions and disturbance on the body pitch angle

Once the TWIP is stabilized, an external force is applied to the body pitch angle, in order to test the response to disturbances.

Assuming that the initial states are:

$$x_o = [0 \quad 0.1 \quad 0 \quad 0]^T \tag{66}$$

The next figures show the responses, when each controller is used.

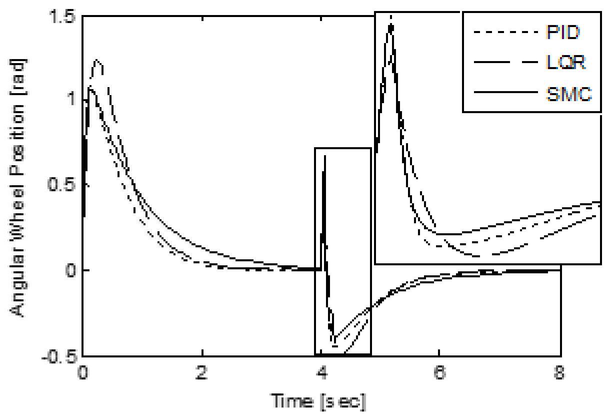

Fig. 11 TWIP, angular wheel position response

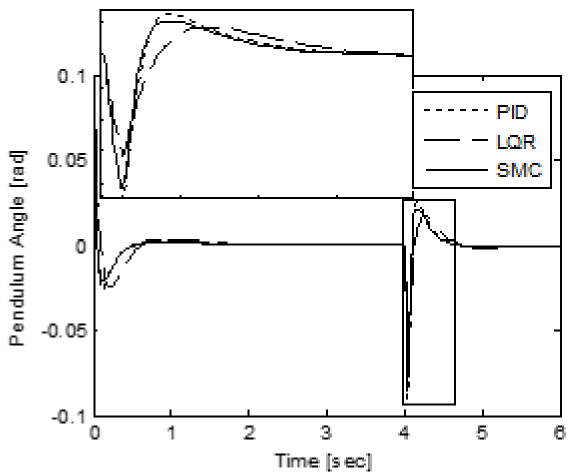

Fig. 12 TWIP, body pitch angle response with an external force applied.

In fig. 12 the SMC response is faster than LQR and it has a smaller overshoot than PID, when the controllers are tested with a disturbance.

In figures from 5 to 12, there is no chattering present, because of the filter.

Table 4. ISE Comparison of three controllers with disturbance

	PID	LQR	SMC
	$ISE * 10^{-3}$		
ψ	0.666	0.622	0.572
θ	653.2	947.9	768.2

5 Conclusion

The three controllers were developed and compared by simulations.

The SMC presented the best ISE for both cases, without disturbances and with disturbances.

From implementation point of view, LQR and SMC are easy to design, and PID does not need a model to be tuned.

The Two-wheeled Inverted Pendulum is a good teaching tool for learning conventional and modern control strategies implementation.

ACKNOWEDGMENTS

Oscar Camacho thanks PROMETEO project of SENESCYT. Republic of Ecuador, for its sponsorship in the realization of this work.

References:

[1] K. Lundberg, T. Barton, History of Inverted-Pendulum Systems, *8th IFAC Symposium on Advances in Control Education*, 2009.
[2] Z. li, C. Yang, L. Fan, *Advanced Control of Wheeled Inverted Pendulum Systems*, © Springer-Verlag, 2013.
[3] K. Ogata, *Modern Control Engineering*, Prentice Hall, 2010.
[4] A. N. K. Nasir, M. A. Ahmad, R. M. T. Raja Ismail, The Control of a Highly Nonlinear Two-wheels Balancing Robot: A Comparative Assessment between LQR and PID-PID Control Schemes, *International Journal of Mechanical, Aerospace, Industrial, Mechatronic and Manufacturing Engineering*, Vol:4, No.10, 2010.
[5] F. Grasser, A. Arrigo, S. Colombi, A. C. Rufer, JOE: a mobile inverted pendulum, *IEEE Trans. Industrial Electronics*, Vol.49 (1), No.1, 2002, pp. 107-114.
[6] J. Huang, H. Wang, T. Matsumo, T. Fukuda, K. Sekiyama, Robust Velocity Sliding Mode Control of Mobile Wheeled Inverted Pendulum

Systems, *International Conference on Robotics and Automation*, 2009.

[7] K. Pathak, J. Franch, K. Agrawal, Velocity and position control of a wheeled inverted pendulum by partial feedback linearization, *IEEE Trans. Robotics,* Vol.21 (3), No.3, 2005, pp. 505-513.

[8] M. Herrera, W. Chamorro, A. Gómez, O. Camacho, Two Wheeled Inverted Pendulum Robot NXT Lego Mindstorms: Mathematical Modelling and Real Robot Comparisons, *Revista Politécnica*, Vol.36, No.1, 2015.

[9] Y. Yamamoto, Nottaway-GS Model Based Design – Control of self-balancing two-wheeled robot built with LEGO Mindstorms NXT, *http://www.mathworks.com/matlabcentral/fileexchange/loadFile.do?objectId=13399&objectType=file*, 2008.

[10] M. Herrera, Modelado Discreto y Control Óptimo de Sistemas No Lineales Multivariables y su Aplicación a un Péndulo Invertido utilizando Lego Mindstorms, *Master of Science Thesis,* Universidad Politécnica de Madrid, España 2014.

[11] B. Kuo, *Sistemas de Control Automático*, Pearson Education, 1996.

[12] B. M. Al-Hadithi, A. Jiménez, J. D. L. Delgado, A. J. Barragán, J. M. Andújar, Diseño de un Controlador Borroso Basado en Estructura Variable con Modos Deslizantes sin Chattering, *Simposio CEA de Control Inteligente,* 2014, pp.1-4.

[13] Y. Pan, K. Futura, S. Suzuki, S. Hatakeyama, Design of Variable Structure Controller – From Sliding Mode to Sliding Sector - , *39th IEEE Conference on Decision and Control*, 2000.

[14] P. Kachroo, M. Tomizuka, Chattering reduction and error convergence in the sliding-mode control of a class of nonlinear systems, *IEEE Trans. On Automatic Control,* Vol.41, 1996, pp.1063-1068.

[15] D. Gu, P. Petkov, M. Konstantinov, *Robust Control Design with MATLAB®*, chapter 19, © Springer-Verlag, 2013.